Re-visiting the mass-flux model for Explosive Reactive Armor and the effect of plate thickness

Meir Mayseless, S. Friling, L. Misiuk

PII: S2214-9147(19)30276-4

DOI: https://doi.org/10.1016/j.dt.2019.08.015

Reference: DT 523

To appear in: *Defence Technology*

Received Date: 26 March 2019

Revised Date: 23 July 2019

Accepted Date: 13 August 2019

Please cite this article as: Mayseless M, Friling S, Misiuk L, Re-visiting the mass-flux model for Explosive Reactive Armor and the effect of plate thickness, *Defence Technology* (2019), doi: https://doi.org/10.1016/j.dt.2019.08.015.

Re-visiting the Mass-Flux Model for Explosive Reactive Armor and the Effect of Plate Thickness

Meir Mayseless[1], S. Friling[2], L. Misiuk[3]

[1] Ben-Gurion University, Beer-Sheva, 84105, Israel. meir.mays@gmail.com
[2] Rafael, P.O. Box 2250, Haifa, Israel, frils@rafael.co.il
[3] Matmon Unit, Technological Division, Mil. P.O. Box 01154, IDF, Israel, levmi1@gmail.com

Corresponding author: Meir Mayseless

Re-visiting the mass-flux model for explosive reactive armor and the effect of plate thickness

ABSTRACT

Explosive Reactive Armor was originally modeled under the assumption that the plates in the cassettes were very thin. Hence their thickness could be ignored, and the thicknesses of the plates were considered only based on their areal mass density. In particular, it was assumed that the jet-plate interaction was controlled by the plates to jet-mass-flux ratio criteria for a specific jet velocity and diameter. In the present study, we extended this analysis, examining the effect of the variation of the mass-flux along the jet on the disruption effect by the two plates. In addition, we examined the thickness effect of the plates on the plate's effectiveness, replacing the steel plates by low-density materials like aluminum and polycarbonate. The mass-flux model was adjusted to account for the plate-thickness effect. It was found that increasing the thickness of the plate, keeping the areal weight unchanged, slightly increases the overall effectiveness of the cassette, in particular by the forward moving plate interacting with the center and the slow parts of the jet.

Keywords: explosive reactive armor, armor, shaped-charges, jet disruption

1. Introduction

Explosive Reactive Armor (ERA) is usually composed of an explosive layer in between two metal plates, generally made of steel. A schematic configuration of an explosive reactive cassette is presented in Fig. 1. The cassette is usually positioned at an oblique angle to the jet path. The plate that is being hit first moves towards the jet and its velocity vector opposes that of the jet, which is called the Backward Moving Plate (BMP). The second plate moves in the jet direction and is therefore named the Forward Moving Plate (FMP). These names are given to discriminate between the two plates: Which is the first plate between the one that is being hit first and the one that is placed first in the cassette. Since we have a natural positive direction that is presented by the incoming jet, we chose to use this direction also for the plate names.

In 1984, 35 years ago, the first theoretical paper explaining the mechanisms by which ERA defeats shaped-charge jets was presented [1]. Several physical mechanisms were revealed in that paper for the first time, including the hydrodynamic mass-flux model and the different rules for the two metallic plates, the FMP and BMP.

Each plate has a different relative velocity to the incoming jet. Hence the interaction velocity, as well as the interaction time interval between each jet element and the plate, is different. The blast mechanism that usually deflects the fast parts of the emerging jet was explained and proved experimentally in this first paper as well [1]. Another pertinent observation in the study was the so-called "Pebble-Stone Model," proposed to explain the emerging jet tip and the periodic nature of the jet–plate interaction. Lastly, the deflection nature of the BMP that causes the jet to deviate from its original velocity direction once the jet-plate's relative velocity is high was presented.

The large hole created by the head-on interaction of the jet tip, while penetrating the cassette before the plates start to move, and the plates' strips that interacts sideways with the rest of the jet are presented in references [2-5].

The jet is typically composed of several parts, including the tip, which moves ahead of the main jet at a speed of 7~10 km/s, and for a point intiated charge is wider than the slower parts of the jet that follows, as seen, for example, in Fig.2 [6,7]. The jets usually move straight with a velocity gradient that causes them to stretch between the tip and the tail, which moves at a typical velocity of 2 km/s to 3 km/s. The slowest part of the jet is the massive slug, which moves far behind the jet at a typical velocity of about 0.5 km/s. Between the slug and the tail, we always find the Appendix, a disturbed part that contributes to penetration only in special cases [7].

As soon as the tip of the jet hits the cassette, the explosive is detonated, causing the metallic plate to move aside. The parts of the jet that interact with the moving plates are deflected and perturbed, as shown schematically in Fig. 3 and in an X-ray test in Fig. 4. The front part of the jet that interacts first with the BMP and later with the FMP is severely perturbed and undulated downwards (in our presentation), while the slower part of the jet, which in this schematic illustration and test, interacting only with the BMP, is mainly deviated upwards. The rear parts of the jet, the Appendix, and the slug do not interact with the ERA in the test presented in Fig. 4. The illustration of the upwards movement of the part of the jet that interacts only with the BMP is somewhat exaggerated in Fig. 3, as seen in Fig. 4, to indicate the main effect of the BMP.

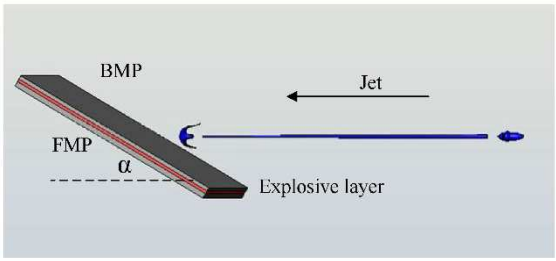

Fig. 1. Schematic view of a reactive cassette just before being hit by a jet.

The plates' velocity is usually one order of magnitude lower than that of the tip of the jet, and since the jet is usually thin, the craters created in the plates during the sideways interaction are also small. Therefore, the final hole shapes in the plates have a "key" hole shape, as illustrated in Fig. 3 and were found experimentally [3]. The mass that was in the thin and long parts of the craters in the plates were named the strips. The strip mass directly interacts with the jet.

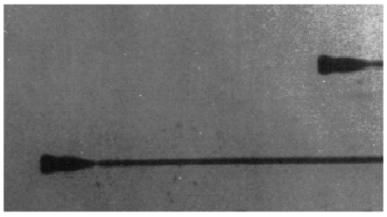

Fig. 2. Two radiographs of a massive jet tip of a 60º point initiated charge, nicely showing the tip of the jet emerging soon after the liner collapse process ended.

It was therefore hypothesized that the interaction between the main part of the jet and the plates could be regarded as an interaction between two streams: the jet and the strip. The mass-flux ratio of the two will determine the effectiveness of the ERA. Detailed consideration of the mass-flux distribution of the jet throughout the entire interaction process was missing. That information will be presented in the following sections, and the benefits that are formed by the plate thickness will also be addressed.

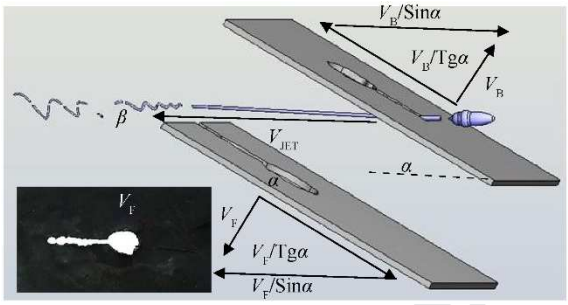

Fig. 3. Schematic view of an ERA cassette interacting with a shaped charge jet, and a plate that was found in one of the tests (left-bottom corner).

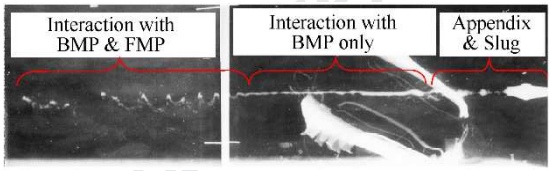

Fig. 4. X-Ray picture of a point-initiated shaped-charge jet interacting with a symmetric 1.6 mm/3 mm/1.6 mm [30º] steel cassette, representing the various interaction zones.

2. JET MASS-FLUX

Moving from tip to tail (excluding the massive tip, the Appendix, and the slug), the velocity of the jet decreases while its diameter increases. Freezing the jet at a given moment (Fig. 5 for example), the change in the mass-flux of the jet emerging from a 60º point initiation charge [6] computed by the M-SCAN code [8] is presented in Fig. 6. This is the mass-flux (or momentum) distribution for a fixed time as a function of the jet velocity, normalized by the mass flux of the first jet particle behind the massive tip. The MKS units of the mass flux are kg·m/s.

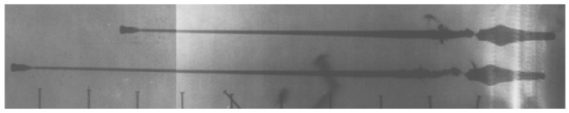

Fig. 5. X-ray picture of a point initiated shaped-charge jet [3].

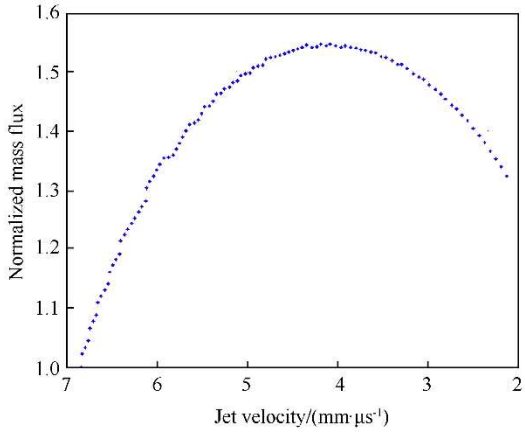

Fig. 6. Normalized mass-flux distribution of a continuous jet emanating from a point-initiated charge at 120μs.

As shown, moving from tip to tail, the mass-flux increases first, up to the jet velocity of about 4.2 km/s, and then decreases. The mass-flux at the tail is smaller by about 15% compared to that at the maximum point, and it is about 30% greater than that close to the tip. The massive tip is not taken into account at this point since it erodes during the penetration through the plates and the detonation processes at the initial impact before the actual jet interaction with the moving plates.

Hence, according to the mass-flux considerations, the zone in the jet that is the hardest to be disrupted (lowest cassette efficiency) is its center one. The next hardest zone for disruption (modest cassette efficiency) is the slow part of the jet, while the easiest part to disrupt (highest cassette efficiency) is the fast part of the jet. This mass-flux consideration overlooks two main problems, which are solved differently. The main problem to disrupt the fast part of the jet is the acceleration time of the plates (an effect that is being compensated by the expanding detonation products) and the main problem to disrupt the tail of the jet are the edge effects.

Assuming that the thickness of the plates can be overlooked and that the plates are long enough, the interacting length rate of the strip, $\dot{l}_{\mathrm{p}}$, and the length rate of the jet, $\dot{l}_{\mathrm{j}}$, which interact at a given time interval, are

$$\dot{l}_{\mathrm{p}} = V_{\mathrm{p}}/\mathrm{tg}\alpha \qquad \dot{l}_{\mathrm{j}} = V_{\mathrm{j}} \pm V_{\mathrm{p}}/\sin\alpha \qquad (1)$$

where the (+) sign is for the BMP and the (-) sign is for the FMP. V_{j} and V_{p} are the jet and plate velocities respectively, and α is the orientation of the plates relative to the jet's original path. To calculate the mass-flux, one needs to multiply each of these terms by the mass per unit length at the interaction zone, taking into account the change in the dimensions of the interacting parts. The mass per unit length of the plate can be considered constant (see also Eq. (6)), but the mass per unit length of the jet changes with time and point of interaction, as is shown below.

Since the jet is moving, the mass-flux of the jet arriving at a given target (distance is fixed) is somewhat different than that presented in Fig. 6, and it is

presented in Fig. 7. It takes about 100 μs for the jet to pass through the plate located at 3CD, with a large variation in disruption in the jet mass-flux.

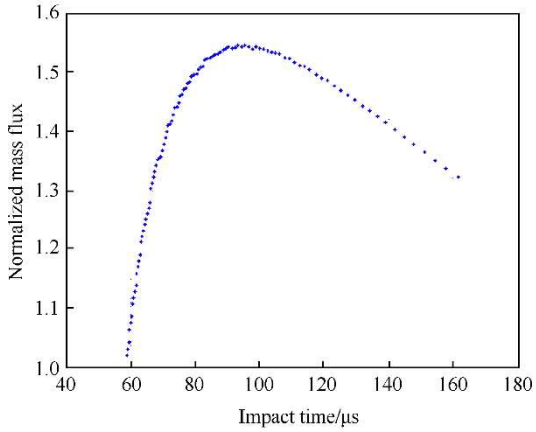

Fig. 7. Normalized mass-flux of a point-initiated jet at 3CD stand-off, as a function of time measured from initiation.

If the target is moving, as in the case of an ERA, the radius of the jet that interacts with the moving plates is different for each one of the plates, as presented in Fig. 8, for a cassette where each plate is moving at a speed of 800 m/s in 30º obliquity. The M-SCAN calculations are for a continuous jet and an infinitely long cassette. For each of the plates, there are red dots that mark the last jet element that interacts with the plate, depending on its dimensions.

The whole jet interacts with the BMP, as long as the interacting length permits a 99 mm strip, so the entire jet and part of the Appendix are expected to be interfered with. The jet velocity at the end of this interaction is the tail velocity, hence, 2130 m/s. The diameter of the jet at this point is about 4.25 mm.

The interaction with the FMP stops according to the allowed strip length. If the strip is 200 mm long, the last jet element that interacts with the FMP has a velocity of 3050 m/s and a diameter of 2.3 mm. If the strip length is 100mm long, the last jet element that interacts with the FMP has a velocity of 4080 m/s, and the diameter of the jet at this point is 2.47 mm. The slower parts of the jet will interact only with the BMP in this case.

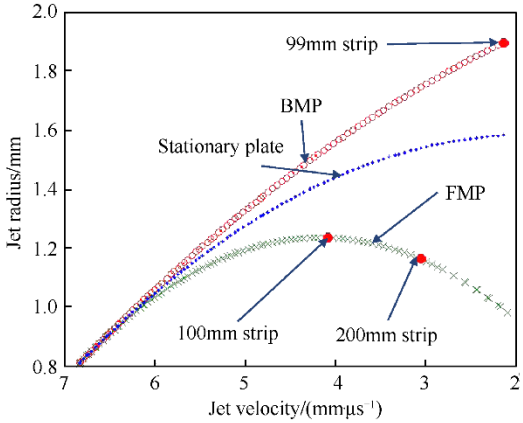

Fig. 8. The jet radius of a point-initiated charge interacting with an FMP (green crosses), a BMP (red dots) moving at a speed of 800 m/s, and a stationary plate (blue dots) as a function of the jet velocity. The initial stand-off is 3CD.

The two red dots on the FMP curve represent the points where the 200 mm and 100 mm strip end their interaction.

If the jet breaks before interacting with the plates, the radius of the drops remain constant, and the decrease in the radius of the jet interacting with the FMP differs from the one presented in Fig. 8, especially for the slow part of the jet.

Based on the radiuses that are presented in Fig. 8, the jet mass-fluxes interacting with the BMP and the FMP are calculated, taking into account the radiuses of the jet at the moment of interaction with the plates. The mass-flux of the plates entering the interaction zone is constant. Hence, we should expect variations in the jet disruption efficiency by the plates, as was presented in Ref. [1]. The calculations in Ref. [1] were for a momentary event. Taking the mass-flux changes along the jet, the jet radiuses and velocities, we can calculate the plates ideal disruption efficiency for each part of the jet, as shown in Fig. 9, for an ideal case in which the plates move at a constant velocity.

Taking the plate's acceleration time into account (not shown here, but presented later in this article), the efficiency of the plate changes close to the jet's fast parts, starting with a very low efficiency because of the acceleration period, which increases and meets the ideal efficiency curve, as will be explained below.

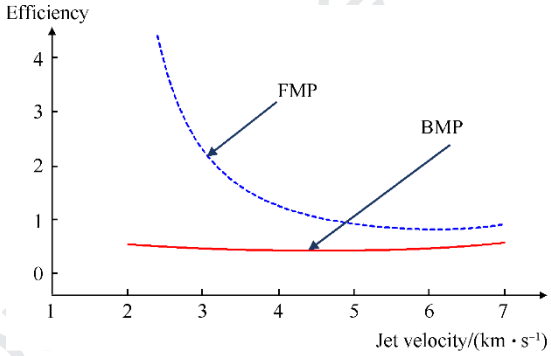

Fig. 9. The plates efficiency (plate to jet mass flux, Eqs. 4-5) as a function of jet velocity assuming the plates are moving at a velocity of 800 m/s.

The BMP efficiency is almost constant. It decreases by about 25% at the center of the jet compared to the tip at a jet velocity of about 4.5 km/s and increases back at the tail. The BMP efficiency is less affected by the jet properties compared to that of the FMP. Ignoring the acceleration process, the disruption efficiency of the FMP at the jet tip is about 50% higher compared to that of the BMP. The main reason for that is the relative velocity difference between the two plates. As we move backwards along the jet, towards the tail, the dominancy of the FMP becomes evident. In particular, it should be noted that the FMP is extremely efficient against the slower parts of the jet. Typically, these parts of the jet do not interact with the FMP.

If we examine the disrupted jet in Fig. 4, we can see that the FMP is very effective up to the center of the jet where it stops interacting with the jet because of edge effect. In contrast to the FMP, the disruption of the jet by the BMP is

very weak, especially close to the rear parts of the jet, as expected by the analysis presented in Fig. 9.

The acceleration phase of the plates in the test that is presented in Fig. 4 is very short in time. Assuming a one-dimensional expansion, the acceleration distance and time can be approximated according to [9].

$$V = V_{\text{final}}[1 - \left(\frac{x_0}{x}\right)^2]^{0.5} = V_{\text{final}}\frac{t}{\tau}[\left(\frac{t}{\tau}\right)^2 + 1]^{-0.5} \qquad (2)$$

V_{final} is the final plate velocity, x_0 is the explosive thickness divided by 2 (symmetric cassette), x is the plate position, t is the time, and τ is a time constant equal to half the explosive thickness divided by final plate velocity. Hence, the acceleration period is about 10 µs, out of an average interaction time of 100µs, according to Fig. 7. The fast parts of the jet are therefore interacting mainly with the exploded product flow [1, 10], downstream from the penetration and gas flow, and appear as an interaction with the FMP [1].

It should be noted that the BMP interacts with whole of the jet, even for a 200 mm cassette, while the FMP interacts only with part of the jet.

3. Plate thickness effect

In most of the studies where the thicknesses of the plates were changed, the explosive thickness was kept constant. Hence, two parameters were changed at the same time, plate thickness and plate velocity (see Ref. [11]). In the present study, we didn't change the weights of the plates or the explosive, but we changed material density. Changing the materials of the plates to low density materials, aluminum, for example, creates a larger interaction zone since the interacting plates are much thicker. On the other hand, the craters in the aluminum plates are usually greater compared to that in the steel plates because of the lower yield strength, the larger thickness, and the faster crater opening. Keeping the areal density constant, the mass-flux of the plates stay the same, but the plate mass-flux per unit length of the jet changes. The lower the plate density, the smaller the mass-flux per unit jet length, and the question is how it will affect the jet disruption process.

Four experiments were conducted to examine the plate material density effect. The X-ray pictures for the four tests are presented in Figs. 10–13. In all the experiments, the mass of the plate per unit area was the same, and the jets hit the cassette at about one third of its length measured from the bottom. The symmetric cassettes contained 1.6 mm mild steel, 4.8 mm soft aluminum, 4.8 mm hard aluminum, or 10 mm polycarbonate (PC) for each of the plates.

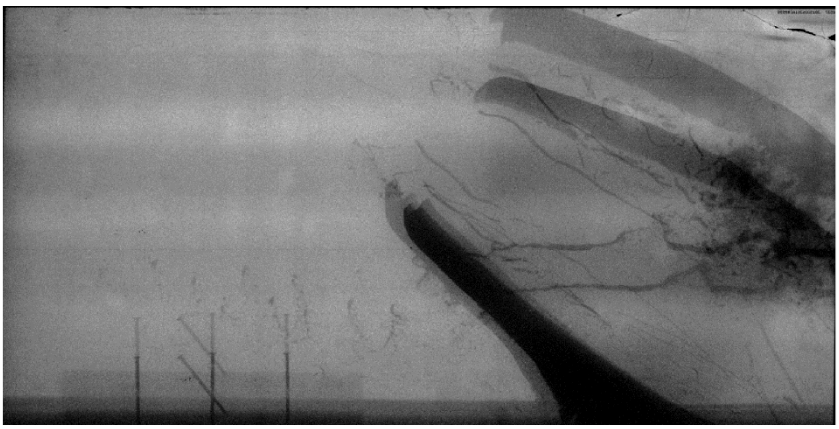

Fig. 10. X-ray picture of a jet interacting with a steel plate cassette at 71 µs and 86 µs.

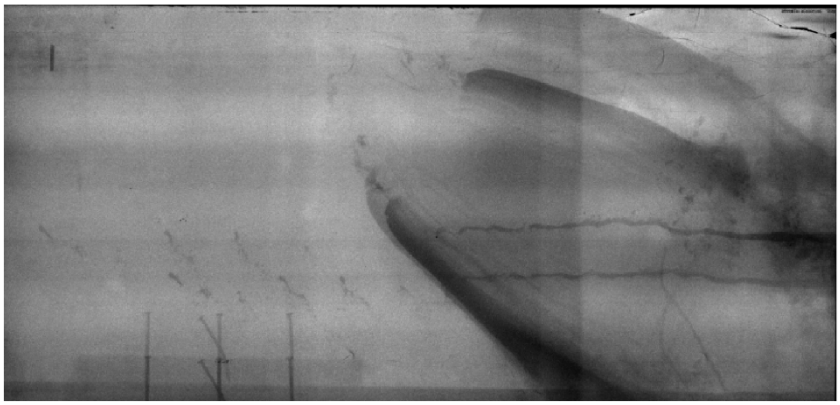

Fig. 11. X-ray picture of a jet interacting with a hard 6061-T6 aluminum plate cassette at 71 µs and 86 µs.

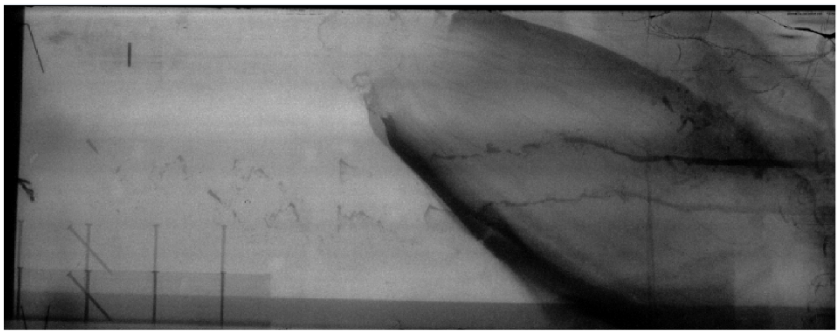

Fig. 12. X-ray picture of a jet interacting with a soft 5052 aluminum plate cassette at 71 µs and 86 µs.

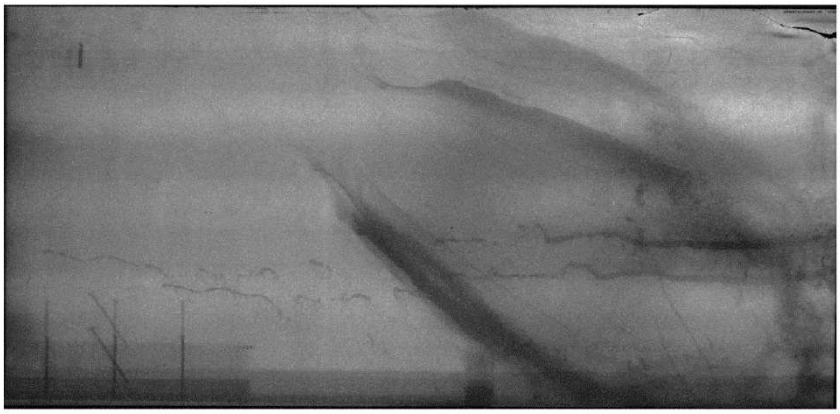

Fig. 13. X-ray picture of a jet interacting with a PC plate cassette at 71 μs and 87 μs.

The residual penetration into an RHA witness plate in all four tests was close. The deepest crater, in the steel cassette test, was 23 mm, compared to 13~16 mm for the aluminum cassettes and 25 mm for the PC one. The aluminum cassette is therefore better then the steel one by about 6%, while the PC cassette has about the same efficiency as the steel one.

It is interesting to note that the overall shapes of the disrupted jets interacting with the steel and the aluminum cassettes were similar. The first fast element of the jet that emerges from the cassettes, in all the tests, is tilted, mainly because of the explosive product flow effect. The fast acceleration of the steel helps to disrupt the jet tip. The sound speed in aluminum is high, but because of the greater thickness, the acceleration period of the aluminum plates is somewhat longer compared to the thin steel plates. In addition, the larger crater in the aluminum plates left a longer but tilted jet tip, which does not contribute to deeper residual penetration. Comparing the two aluminum cassettes, only a small difference in the disrupted jets after the interaction with the FMPs is observed. The deflected jets after the interaction with the two aluminum BMPs are somewhat different. At this point, we don't know why. The main results are that the aluminum cassettes provide somewhat better efficiency compared to steel.

The acceleration effects in the PC plates are much slower due to the slower sound speed of the PC and its greater thickness. The interaction of the jet with the moving plates (the strip) is delayed, and the tip is longer, although tilted by the flow of the detonated explosive products.

In all the cases, we observed a strong local interaction between the rear part of the jet and the plate caused by the BMP interaction with the jet.

The strength of the plates affects the craters at the interacting area if the impact velocity is lower than about 3 km/s, as was shown for high hardness aluminum (V-95, density of 2.8 g/cm^3) and titanium (VT-6, density of 4.5 g/cm^3) in Ref. [12]. For higher impact velocities, the interaction is considered hydrodynamic. Hence, we can assume that the jet-plate interaction is hydrodynamic for almost all jet elements (although the late flow of the craters in the plates is affected by its material strength), and we should not see a major difference between the two aluminum tests, as was indeed found.

Assuming a hydrodynamic penetration, the emerging new jet tip can be calculated [13], and it is well known that for the same target weight, the lower the target density, the lower the new tip, reducing the perturbed jet effectiveness.

If we take into account the plate thickness, *h*, and the actual time interval the jet interacts with the plates from the moment it starts to interact with each plate until it stops, assuming that the plates are moving at a constant speed during the interaction period, the jet interacting lengths are

$$l_{\mathrm{j}} = [(V_{\mathrm{j}} \pm V_{\mathrm{p}} / \sin\alpha)]\mathrm{d}t - h / \sin\alpha \qquad (3)$$

The plate interacting length stays the same in this case, as in Eq. (1). The ratio between the jet interacting length to that of the strip for the two plates can be found in the following equations. Two expressions can be deduced, one based on the strip length and the other on the interacting jet length. Consequently, the mass-flux ratio that is assumed to be a measure for the efficiency, η, of the disruption process is given by Eq. (4) and (5). These equations present the cassette disruption efficiency with respect to each element of the jet.

$$\eta = \frac{\dot{m}_{\mathrm{p}}}{\dot{m}_{\mathrm{j}}} = k\left[\frac{1}{\hat{V}_{\mathrm{P}}}\mathrm{tg}\alpha \pm \frac{1}{\cos\alpha} - \frac{h}{l_{\mathrm{P}}\sin\alpha}\right]^{-1} \qquad (4)$$

or

$$\eta = \frac{\dot{m}_{\mathrm{P}}}{\dot{m}_{\mathrm{j}}} = k\frac{1+h/(l_{\mathrm{j}}\sin\alpha)}{\frac{1}{\hat{V}_{\mathrm{P}}}\mathrm{tg}\alpha \pm \frac{1}{\cos\alpha}} \qquad (5)$$

where

$$k = \left(\frac{\rho_{\mathrm{p}}}{\rho_{\mathrm{j}}}\right)\left(\frac{4\lambda h}{\pi d_{\mathrm{j}}}\right); \qquad \hat{V}_{\mathrm{P}} = V_{\mathrm{p}} / V_{\mathrm{j}} \qquad (6)$$

where ρ_{j} and ρ_{p} are the mass densities of the jet and the plate respectively, d_{j} is the jet diameter, *h* is the thickness of the plate (or strip), and $\hat{V}_{\mathrm{p}}$ is the plate-normalized velocity. λ is a factor of the order of one, which may be used to adjust the width of the strip that interacts with the jet if it is larger than the jet diameter, or, if required, to add plate's strength effects to the interaction process.

The analysis presented above takes into account the strip length (Eq. (4)) or the interacting length of the jet (Eq. (5)), assuming the jet moves at a constant velocity. If h = 0, the two equations will be identical to the old mass-flux equation [1], where the plate-thickness value multiplied by the density is left only in *k* to calculate the areal plate mass.

As we can see from both Eqs. (4)–(5), the thickness of the plate increases the disruption effectiveness. Taking into account the thickness of the plates, the strip's length that interacts with the jet becomes of major importance. The strip lengths are presented in Fig. 14.

The B_strip (the length of the strip of the BMP plate) has a much smaller length compared to the F_strip. The thicker the explosive layer, the faster the BMP moves, and since there is an upper limit to the velocity of the plate, there is also an upper limit to the strip length of the BMP.

The F_strip length increases up to the moment where it exits the plate edge (the edge effect) or its phase velocity exceeds the jet velocity. This edge effect is clearly seen in the x-ray presented in Fig. 4. The higher the FMP velocity, the sooner the edge effect comes into play, although the stronger the jet disruption at each point of interaction.

It is assumed that the longest strip length is 200 mm (a constant that is determined by the cassette length), and the lengths are normalized by this value. The normalized F_strip length increases up to one when the explosive thicknesses in the two cassettes are about 5.2 mm and 4.9 mm for tip velocities of 5.7 km/s and 6.2 km/s, respectively. The F_strip is always longer than the B_strip, and this is one of the reasons for its greater effectiveness besides the effectiveness sensitivity to the FMP edge effect. It may well be that the B_strip will continue to interact with the jet long after the F_strip is no longer effective. The higher the tip velocity, the longer the strip for a given explosive thickness, but the stronger the edge effect (after increasing the explosive thickness). Reducing the density of the plates decreases the new jet tip, another benefit of the low-density plates, as was explained above.

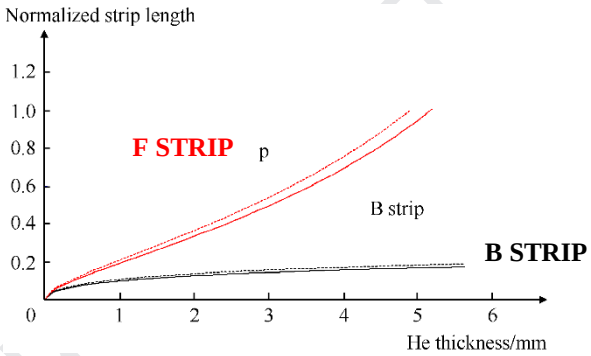

Fig. 14. Normalized strip length as a function of HE thickness, for a symmetric 3/x/3 [30º] steel cassette (broken lines) and for 8.6/x/8.6 [30º] aluminum cassette (solid line).

It should be noted that since the FMP stops interacting when the HE thickness is greater than 5.2 mm, the only plate that disrupts the jet is the BMP from that point on.

Calculating the interaction efficiency, Eqs. (4) and (5), taking into account the thickness of the plates, we find that the efficiency is strongly affected by the FMP and less affected by the BMP, as shown in Fig.15. This improved efficiency, due to the increased FMP thickness, is probably the main effect that causes the aluminium cassette to be better compared to the steel one in the experimental results that were presented above.

Moreover, the main affected parts of the jet are its center and slower parts. Hence, taking into account the FMP thickness effect, it seems that we can use slower velocities to improve the edge effect without losing disruption efficiency.

The efficiencies during the plates' acceleration phase are also presented in Fig. 15, according to Eq. (2). The acceleration affects the efficiency of the fast part of the jet only from the tip that starts the initiation up to about 6 km/s. The

thinner the plate, the shorter the acceleration phase and the smaller the fast part of the jet that is not affected by the interaction with the plates, as seen in the experimental results.

To compare the efficiencies of various cassettes we have to integrate the efficiencies along the jet. By doing so, assuming, for simplicity, that all parts of the jet touch and interact with the plates, we find that the aluminium cassette is expected to be better compared to the steel one by about 3%, close to the experimental observation.

It is expected that including the acceleration phase at this point will not change much these results since the fast part of the jet is strongly disrupted by the detonation products.

Our theoretical analysis predicts that the efficiency of the PC cassette will be much better compared to the steel one, unlike the experimental result. More tests are needed to explain these results.

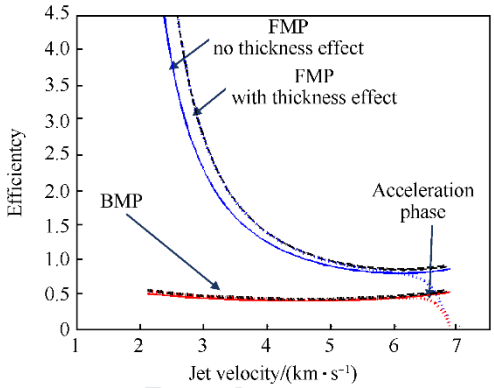

Fig. 15. FMP (broken black and solid blue lines) and BMP (doted black and solid red lines) efficiency for 8.6 mm [30º] aluminum cassette, including the acceleration phase.

4. SUMMARY

The mass-flux model for the explosive reactive cassette was explained and extended into an analytic model that enables us to estimate the effect of the various physical parameters, like the orientation, plate velocity, plate thickness, plate length and plate acceleration phase, on the disruption efficiency of each part of the shaped-charge jet.

The different role of the two plates, the FMP and the BMP, in disrupting the jet was explained, taking into account the strip lengths and the thicknesses of the two plates. Keeping the weight of the cassette constant, it was found that lowering the density of the two plates is beneficial in disrupting the jet. The main benefit of the BMP is the smaller strip, hence, smaller edge effects, while the main advantage of the FMP emanates from the efficient interaction with the center and rear parts of the jet. The emerging tip of the jet is usually deflected by the flow of the explosive products.

The new model was examined experimentally, comparing a steel cassette to an aluminum one, and by facilitating understanding of the role of the various

interaction parameters involved. To understand the reasons for the relatively low efficiency of the thick PC cassette more tests are needed.

Acknowledgement

This work is supported by the Israeli MOD/DDR&D.

REFERENCES:

[1] Mayseless M., Ehrlich Y., Falcovitz Y., Weihs D., and Rosenberg G., Interaction Of Shaped Charge Jets with Reactive Armor, In Proceedings of the 8th Int. Sym. on Ballistics, 1984, Orlando, FL, pp.VII-15-VII-20.

[2] Mayseless M., Effectiveness of Explosive Reactive Armor, J. Appl. Mech. 2011, 78(5), 051006-1 to 051006-11, doi:10.1115/1.4004398.

[3] Mayseless M., Jet Plate Interaction: The Precursor, In Proceedings of the 18th Int. Sym. on Ballistics, 1999, San-Antonio, TX, Vol. 2, pp. 1019-1026.

[4] Mayseless M, Marmor E., Gov N., Kivity Y., Falcovitz J., and Tzur D., Interaction of a Shaped Charge Jet with Reactive or Passive Cassettes, In Proceedings of the 14th Int. Sym. on Ballistics, 1993, Quebec, Canada, Vol. 2, pp. 439-448.

[5] Held M., Mayseless M., and Rototaev E., Explosive Reactive Armor, In Proceedings of the 17th Int. Sym. on Ballistics, 1998, Midrand, South Africa, Vol.1, pp. 33-46.

[6] Mayseless M., Hirsch E., Lindenfeld A., and Me-Bar Y., Jet Tip and Appendix Characteristics Dependence on Liner Thickness in 60° Point Initiated Shaped Charge, In Proceedings of the 17th Int. Sym. on Ballistics, 1998, Midrand, South Africa, Vol.2, pp. 187-195.

[7] Mayseless M. and Hirsch E., The Appendix, In Proceedings of the 24th Int. Sym. on Ballistics, 2008, New Orleans, LA, pp. 1069-1076.

[8] Hirsch E., SCAN, Shaped Charge Analyzer Model Computer Program User Manual, Ver. 1. Prepared by E. Hirsch, Drew Goodlin, and T.R. Sharon, Southwest Research Institute, 1998, San Antonio, TX.

[9] Flis W. J., A Lagrangian Approach to Modeling the Acceleration of Metal by Explosives, in Proceedings of the 17th South-Eastern Conference on Theoretical and Applied Mechanics, 1994, Hot Springs, AK.

[10] Mayseless M. and Asaf Z., Jet Interaction with High Explosive Flow, In Proceedings of the 27th Int. Sym. on Ballistics, 2013.

[11] Micković D., Jaramaz S., Elek P., Miloradović N., and Jaramaz D., A Model for Explosive Reactive Armour Interaction with Shaped Charge Jet, Propellants, Explosives, Pyrotechnics, 2016; 41:53-61. https://doi.org/10.1002/prep.201500163.

[12] Gooch W. A., Burkins M. S., Walters W. P., Kozhushko A. A., and Sinani A. B., Target Strength Effect on Penetration by Shaped Charge Jets, Int. J. Impact Engng. 2001; 26:243-248, https://doi.org/10.1016/S0734-743X(01)00083-5.

[13] Mayseless M. and Genussov R., Jet Penetration into Low Density Targets, HVIS 98 Huntsville, AL, 16-19 Nov., 1998.